Preparation of PS-*g*-PA6 Copolymers by Anionic Polymerization of ε-Caprolactam Using PS Precursors with *N*-Carbamated Caprolactam Pendants as Macroactivators

Yao-Chi Liu,[1,2] Wei Xu,[1] Yuan-Qin Xiong,[3] Wei-Jian Xu[1]

[1]*Institute of Polymer Science and Engineering, Hunan University, Changsha 410082, China*
[2]*College of Urban Construction, Nanhua University, Hengyang 421001, China*
[3]*College of Chemistry and Chemical Engineering, Hunan University, Changsha 410082, China*

Received 24 August 2007; accepted 27 December 2007
DOI 10.1002/app.27965
Published online 29 February 2008 in Wiley InterScience (www.interscience.wiley.com).

ABSTRACT: The graft copolymer of polystyrene and polyamide 6 (PS-*g*-PA6) was investigated by anionic polymerization of ε-caprolactam (CL), using the free radical copolymer of styrene and a kind of allyl monomer containing *N*-carbamated caprolactam group as macroactivator (PS-CCL). CL monomers were grafted onto PS-CCL backbone via initiating *N*-carbamated caprolactam (CCL) pendants along its backbone to form the graft copolymer in the presence of catalyst sodium caprolactamate. The macroactivator was characterized by Fourier-transform infrared spectroscopy and nuclear magnetic resonance, and the graft copolymer by the selective solvent extraction technique using methanol and chloroform as solvents. PS-*g*-PA6 copolymers with different PS content were synthesized to study the effect of PS on morphology, crystallinity, dimensional stability, and thermal properties, using scanning electron microscopy, X-ray diffraction, water absorption measurement, thermogravimetric analysis, and differential scanning calorimetry. The results show the percentage crystallinity of graft copolymer decreases with increasing PS content, but the addition of PS scarcely influences the crystalline structure of PA6. The graft copolymer has improved thermal properties and dimensional stability. © 2008 Wiley Periodicals, Inc. J Appl Polym Sci 108: 3177–3184, 2008

Key words: polyamide 6; polystyrene; graft copolymer; water absorption; thermal properties

INTRODUCTION

The usage of polyamide is limited by some drawbacks, such as high moisture absorption, low dimensional stability, and low thermal degradation temperature. Rigid organic filler toughening, composed of a ductile polyamide matrix and rigid dispersed brittle particles, is an important method for the modification of polyamides. Rigid polymers, such as polystyrene, poly(methyl methacrylate), and polyimide, are now readily available.[1–10] Among the above combinations of brittle/ductile polymers, the polyamide/polystyrene system shows the poorest miscibility and least interfacial adhesion between the two phases because of unfavorable interactions of polar polyamide and nonpolar polystyrene at the molecular level.[7] For linear polyamides, the miscibility of polyamide/polystyrene can be improved either by addition of a third component (compatibilizer) or by reactive compatibilization (*in situ* formation of copolymers). The aforementioned technologies, however, are not practicable for polyamides prepared by the anionic polymerization of lactams, which commonly results in a high molecular weight (> 50,000), crosslinked, and structural irregular polymer because of Claisen-type condensations and other side reactions.[11,12]

Anionic ring-opening polymerization of ε-caprolactam (CL) is one of the most important commercial processes for producing polyamide 6 (PA6, also known as nylon 6), the versatile material and the most used type of polyamide. During the anionic polymerization, an activator is usually added to speed up the polymerization (activated anionic polymerization) in the presence of a catalyst such as sodium caprolactamate (NaCL), and therefore functionalized PA6 can be prepared by using preformed polymers as macroactivators.[13–15] Instead of reacting the terminal functional groups of linear PA6 (amine and/or carboxylic acid groups) with their polymer component partners, the CL monomers are grafted onto macroactivator backbones. This grafting polymerization route is expected to generate graft copolymers with very high purity.[16] Unlike reactive compatibilization, both the interfacial area limitation and steric hindrance effects are much reduced. Esters,[3] imides[4]

Correspondence to: W.-J. Xu (polymer_group@163.com).

and isocyanate derivatives[10,16] were incorporated into polymers to prepare the aforementioned macroactivators. They can react with CL monomers during the polymerization to form carbamated caprolactam (CCL) moieties from which PA6 chains grow. For an industrial purpose, the activating capacities of esters and imides are relatively low. The time necessary for the completion of polymerization is long (more than 2 h) compared to the mean residence time of a typical monomer cast process (a few minutes). Isocyanate derivatives have higher activating capabilities, but the usage is practically difficult since they are very sensitive to moisture and active hydrogen.

In a previous study, PA6 was grafted onto different rigid polymers via a technical strategy, i.e., fast anionic polymerization of CL activated by the rigid precursors with CCL pendants.[17] Preformed rigid polymers containing CCL pendants were directly used as the macroactivators of anionic polymerization of CL, instead of reacting preformed polymers with CL or NaCL to form CCL moieties during the polymerization. The polymerization took place in a few minutes because of the much lower activation energy for the initial nucleophilic attack of caprolactam anion on the CCL groups.

In this study, the graft copolymers of polystyrene and polyamide 6 (PS-*g*-PA6) with different PS content were investigated. Two grades of PS grafted with CCL (PS-CCL) obtained by free radical copolymerization of styrene and a kind of allyl monomer containing CCL group (ACCL) were used as the macroactivators of anionic polymerization of CL. The ultimate objective is to improve the dimensional stability and thermal properties of PA6. The effect of polystyrene on the morphology and crystallinity of PS-*g*-PA6 copolymer was also investigated.

EXPERIMENTAL

Materials

Styrene was distilled under reduced pressure to remove the inhibitor, and stored in a refrigerator. 2,2′-azobis(isobutyronitrile) (AIBN) was dissolved with methanol, precipitated with chloroform, and dried at 60°C under reduced pressure overnight (mp: 104°C). Toluene was used as the solvent for the radical copolymerization, and purified by distillation in the presence of anhydrous calcium oxide. CL (China Petro and Chem) was recrystallized with acetone (mp: 76–70°C and bp: 268.5°C). Ethanol, methanol, petroleum ether (bp: 60–90°C), phosphorus pentoxide (P_2O_5), dimethylformamide (DMF), chloroform ($CHCl_3$), NaOH, and LiBr were used without further purification. Allyl monomer with carbamated caprolactam moiety (ACCL) was prepared by reacting 2,4-toluene diisocyanate (TDI) with CL and allyl alcohol successively, using dibutyltin diaurate (BZL Reagent) as catalyst.[17] The product was precipitated three times with petroleum ether and dried at 100°C under reduced pressure overnight. Yield 82.9%. mp 41.5°C. FTIR spectrum (KBr): 3335 and 3455 (NH), 2931 and 2859 (CH), 3080, 1711, 1649, and 1596 (amide and imide), 1535 (CC, aromatics), 1395 (=CH), 1214 and 1170 (COC), 844 (=CH), 755 cm^{-1} (CH, aromatics). ^1H NMR spectrum ($CDCl_3$, δ): 7.7–8.1 (1H, Ar—NH—CO—N), 6.9–7.3 (3H, aromatics), 6.6 (1H, Ar—NH—CO—O), 5.9 (1H, C=CH—C), 5.3 (2H, CH_2=C), 4.6 (2H, —CH_2—CO—N), 4.1 (2H, C—CH_2—O), 2.8 (2H, C—CH_2—N<), 2.2 (3H, Ar—CH_3), and 1.9 ppm (6H, lactam). Anal calcd for $C_{18}H_{23}O_4N_3$ (345.33): C 62.55%, H 6.66%, N 12.17%. Found: C 62.47%, H 6.60%, N 12.08%.

Synthesis of PS-CCL macroactivators

PS-CCL macroactivators (Fig. 1, Step 1) were prepared by solution copolymerization of styrene and ACCL at 80°C for 12 h in a 250-mL, three-necked, round-bottom flask equipped with a condenser, a mechanical agitator and a nitrogen inlet tube. AIBN (75 mg, 0.5 mol % to CL monomer) was used as the free radical initiator, and toluene (80 mL) as solvent. The product obtained was precipitated three times with methanol, and then vacuum-dried at 60°C overnight. Two grades of PS-CCL, i.e., PS-CCL58 and PS-CCL112 having 5.8 and 11.2 mol % CCL group, respectively, were used as the macroactivators of anionic polymerization of CL (Table I).

Synthesis of PS-*g*-PA6 copolymers

The PS-*g*-PA6 copolymer was obtained by anionic polymerization of CL, using PS-CCL as macroactivator and NaCL as catalyst (Fig. 1, Step 2). For com-

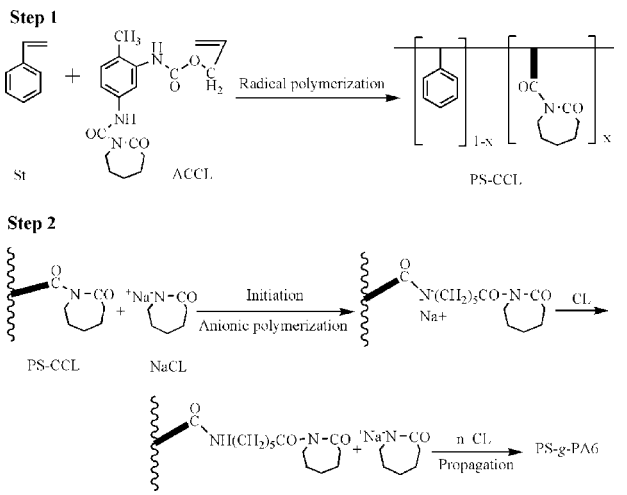

Figure 1 Mechanism of PS-*g*-PA6 graft copolymer formation.

TABLE I
PS-CCL Macroactivators Obtained by Free Radical Copolymerization

Macroactivator	Feed composition by molar ratio	M_n by GPC 10^{-4}(g/mol)	PDI by GPC	Molar fraction of CCL by ^{1}H NMR (%)
PS-CCL112	St/ACCL = 4/1	8.03	2.16	11.2
PS-CCL58	St/ACCL = 9/1	11.9	1.67	5.8

parison, homo-PA6 activated by ACCL was also investigated. The compositions of experimental trials are listed in Table II. The ratio of NaCL to CL was kept constant at 1 mol %. Polymerization was conducted in a heated oil bath whose temperature was monitored by a thermocouple. In a typical synthesis (Trial 3), NaCL component was prepared by reacting CL (8.5 g, 75 mmol) with NaOH (60 mg, 1.5 mmol) at 120°C for 2 h under reduced pressure. PS-CCL112 (0.96 g, containing 0.42 mmol CCL) and CL (8.5 g, 75 mmol) were introduced into an ampoule evacuated and filled with nitrogen several times, and dissolved at 140°C. Then, the NaCL component was poured into the ampoule. The mixed reactants were mixed well in an ultrasonicator at 75°C for 15 min, and allowed to polymerize at 170°C for 20 min.

For analysis, homo-PA6 and PS-*g*-PA6 graft copolymers were firstly cut to pieces, and then grinded in a Thomas Mill at room temperature. The selective Soxhlet extraction using methanol and chloroform as extracting solvents was implemented for all samples.

Measurements

FTIR analysis was performed on a Nicolet Nexus 670 FTIR spectroscopy between 4000 and 400 cm^{-1} in the form of KBr pellets (32 scans, resolution 1 cm^{-1}). ^{1}H NMR spectra were recorded in $CDCl_3$ using TMS as the internal standard on a Hitachi av600 NMR Spectrophotometer. The morphology of polymers was observed using scanning electron microscopy (SEM) on a Hitachi S4700 instrument. The fractured surfaces of the samples were sputter coated with gold to prevent charging in the electron beam. DSC was performed on Perkin-Elmer DSC-7, with a temperature range from 20 to 300°C and sample weight of about 10 mg under nitrogen atmosphere. Samples, encapsulated in aluminum pans, were heated to 300°C at a rate of 40°C min^{-1} and held 5 min at this temperature to cancel their thermal history, then cooled to 20°C at a rate of 40°C min^{-1}. Finally, the sample was reheated to 300°C at a rate of 10°C min^{-1}. The recorded temperatures were calibrated using Indium as standards. Crystalline melting temperature (T_m) was obtained as the maximum of the melting endotherm. Percentage crystallinity (χ_{DSC}) of polymer was calculated via the ratio between the measured and equilibrium heats of fusion ($\Delta H_f/\Delta H_f^0$). The equilibrium heat of fusion (ΔH_f^0) is 230 J g^{-1} for 100% crystalline PA6.[18] XRD were performed on a Rigaku D/Max2500 diffractometer (Ni-filtered, Cu/Kα radiation of wavelength 0.154 nm) in reflection mode over the range of diffraction angles (2θ) from 5° to 45° at ambient temperature. The voltage and tube current were 40 kV and 200 mA, respectively. Percentage crystallinity (χ_{XRD}) was calculated by a standard procedure.[19,20] Thermogravimetric (TG) analysis was performed on a Perkin-Elmer DSC-7. Predried powders (about 2 mg) were heated from 25 to 500°C at 10°C min^{-1} under nitrogen.

RESULTS AND DISCUSSION

Macroactivator synthesis

Synthesized PS-CCL macroactivator was confirmed by FTIR [Fig. 2(a)] and ^{1}H NMR (Fig. 3). As shown

TABLE II
Selected Information of Experimental Trials

Trial	Polymerization system	R_m[a](mol %)	P_w[b](%)	T_p[c]	C_m[d] (%)	Y_p[e] (%)	Remark
1	CL/NaCL	–	–	2 h	–	–	No polymerization detected
2	CL/NaCL/ACCL	0.50	–	20 min	94.2	91.8	Homo-PA6 expected
3	CL/NaCL/PS-CCL112	0.28	3.22	20 min	90.0	86.1	PS-*g*-PA6 expected
4	CL/NaCL/PS-CCL58	0.29	5.30	20 min	89.3	82.5	PS-*g*-PA6 expected
5	CL/NaCL/PS-CCL58	1.16	18.3	20 min	87.9	78.0	PS-*g*-PA6 expected
6	CL/NaCL/PS-CCL58	0.29	5.30	10 min	77.9	73.6	PS-*g*-PA6 expected

[a] Molar ratio of CCL group to CL monomer.
[b] Weight percentage of PS-CCL in polymerization system.
[c] Polymerization time.
[d] Monomer conversion calculated by eq. (2).
[e] Polymer yield calculated by eq. (3).

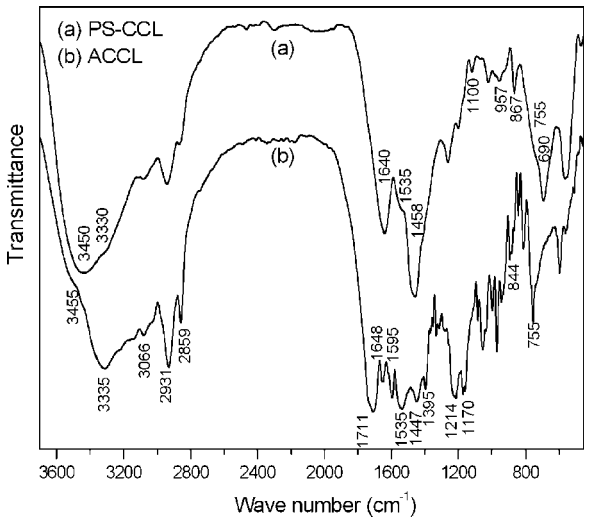

Figure 2 FTIR spectra of (a) PS-CCL58 and (b) ACCL.

in Figure 2(b), the majority of ACCL absorption bands are those corresponding to *N*—H (3335, 3455, 1535), C=O (1648), and C=C (1395, 844 cm^{-1}). For PS-CCL, the bands of *N*—H and C=O appear, but those of C=C disappear; furthermore, it shows all the characteristic bands due to polystyrene, i.e., β(CH) at 1458, γ(CC) at 1100, and γ(CH) at 690 cm^{-1}. Thus, FTIR analysis suggests the formation of PS-CCL macroactivator by free radical copolymerization of styrene and ACCL.

^{1}H NMR results are provided to further confirm the above statement. ACCL exhibits signals of lactam ring protons at δ (ppm) 2.8 and 4.6, and of CH_2=CH—CH_2—O protons at 5.9, 5.3, and 4.1.[17] As shown in Figure 3, PS-CCL exhibits the same signals of lactam ring protons, and that of C—C—CH_2—O at 3.6; however, the peaks at 5.9 and 5.3 ppm for CH_2=CH—C almost disappear. The above results indicate that CCL moieties were incorporated into PS effectively.

Molar fraction of CCL on PS-CCL in Table I and Figure 1, x, could be calculated from the integrated intensity ratio of the C—C—CH_2—O peak at 3.6 ($A_{3.6}$) to the peaks between 6.5 and 8.1 ppm ($A_{6.5–8.1}$) including benzene, NH, and Ar—CH protons.

$$\frac{2x}{5x+6(1-x)} = \frac{A_{3.6}}{A_{6.5-8.1}} \Rightarrow x(\text{mol\%}) = \frac{6A_{3.6}}{A_{3.6}+2A_{6.5-8.1}} \times 100 \quad (1)$$

Note that $A_{3.6}$ in Eq. (1) can be substituted by $A_{4.6}$ (the integrated intensity of CH_2—CO—N peak at 4.6), and also by $A_{2.8}$ (C—CH_2—N< at 2.8 ppm). The x values calculated from various combinations of peaks differ by less than 12%, and the average values are listed in Table I. It is obvious that they are lower than those expected from feed compositions in Table I, indicating the free radical copolymerization of styrene and ACCL resulted in a statistical copolymer with styrene predominance.

Graft copolymer synthesis

Experimental trials carried out in this work are listed in Table II. As one can see CL/NaCL did not polymerize without an activator (Trial 1), but they polymerized when ACCL (Trial 2) and PS-CCL (Trials 3–6) were added as activators. The product of Trial 2 was expected to be a homo-PA6, and those of Trials 3–6 were PS-*g*-PA6 graft copolymers. Figure 1 (Step 2) shows schematically the synthesis of PS-*g*-PA6 graft copolymer: CL monomers are grafted onto the PS-CCL macroactivator via initiating CCL pendants in the presence of catalyst NaCL. It's well known that PS alone cannot function as activator, the CCL pendants helps in funtionalizing PS backbone. In practice, *N*-acetylcaprolactam is the most commonly used fast activator for conventional monomer cast process. The polymerization takes place in a few minutes because of the much lower activating energy for the initial nucleophilic attack of caprolactam anion on the CCL group. Isophthaloyl-biscaprolactam,[20] *N*-carbamoyl-caprolactam[21] and other low molecular weight activators containing CCL group (microactivators) were also reported.[22] The addition of PS-CCL in this study resulted in a polymerization time of less than 20 min. Thus, the activation capacity of PS-CCL macroactivator was similar to that of a microactivator.

Three different analytical techniques were tried to characterize the grafting density and the average PA6 chain length of PS-*g*-PA6 copolymer: NMR, GPC, and selective solvent extraction. The first two were unsuccessful because of the lack of finding

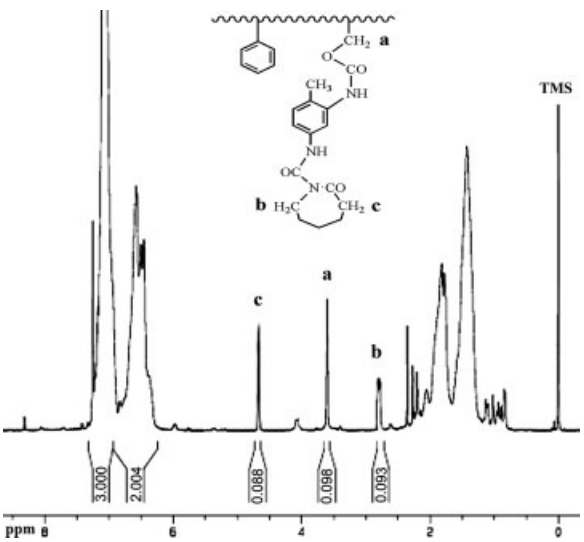

Figure 3 ^{1}H NMR spectrum of PS-CCL58.

good solvents capable of dissolving those polymers, even at high temperature. The selective solvent extraction discussed later provided information supportive of the formation of PS-*g*-PA6 graft copolymer, but it was incapable of estimating the aforementioned factors that determined the ratio of PS/PA6 (PS content). We can only make a rough evaluation based on the feed composition listed in Table II. Compared with Trial 4, Trial 3 is expected to have higher grafting density and lower PS content since the molar fraction of CCL on initial PS-CCL macroactivator is higher. Compared with Trial 5, Trial 4 is postulated to have longer PA6 chain length and lower PS content because of its lower molar ratio of CCL to CL.

Methanol and chloroform were used as the extracting solvents of selective solvent extraction. The former dissolved unreacted CL monomers and cyclic oligomers,[23] and the later dissolved ungrafted PS-CCL macroactivators. After successive extraction, those not dissolved corresponded to graft copolymers. The monomer conversion and polymer yield were calculated using the following equations:

$$\text{Monomer conversion } (\%) = \frac{W_2 - W_1}{W_0 - W_1} \times 100 \quad (2)$$

$$\text{Polymer yield } (\%) = \frac{W_3}{W_0} \times 100 \quad (3)$$

where W_0 is the weight of dried sample, W_1 is the pro rata weight of macroactivator contained in sample, W_2 is the dried weight of sample left after extracting with hot methanol for 16 h, and W_3 is the dried weight of sample left after further extracting with hot chloroform for 4 h.

The data obtained by selective solvent extraction are listed in Table II. In the presence of activator ACCL (Trial 2), CL polymerized with a high degree of monomer conversion. Also, Trials 3–6 activated by PS-CCL macroactivators had quite high monomer conversions, even when the polymerization was artificially terminated after 10 min (Trial 6). Taking one with another, the monomer conversions of Trials 3–5 (graft copolymers) are lower than that of Trial 2 (homo-PA6). As the grafting density decreases (from Trial 3 to Trial 4) and/or the molar ratio of CCL to CL increases (from Trial 4 to Trial 5), the monomer conversion of graft copolymers decreases. It is a logical outcome since the existence of macroactivator in melting CL hinders the movement of CL and the propagation of PA6 chain. For Trial 5, this decrease may also be due to the increase in CCL content. It was reported that the content of cyclic oligomers increased with activator content in the anionic polymerization of CL.[24] The decreasing trend of polymer yield is similar to that of monomer conversion. It is noticeable that some of those products dissolved in chloroform do not necessarily mean that they are not graft copolymers. It could eventually be very rich in PS and very poor in PA6. The above facts seem to be strong enough to show that the anionic polymerization of CL in the presence of PS-CCL yielded graft copolymers with high purity.

The micrographs of polymers examined using SEM give complementary information of PS-*g*-PA6 formation. After successive extraction, the fractured surface of graft copolymer [Fig. 4(b)] is similar to that of homo-PA6 [Fig. 4(a)]. The distribution is quite homogeneous suggests that PS phase was well dispersed in PA6 matrix. If PA6 have not grafted onto PS-CCL backbone, i.e., the final product is a blend of PA6 and PS, discrete holes or domain surfaces left by extracting PS may be seen on the fractured surface because of the low compatibility between PS and PA6 phases.[5,25]

DSC analysis

An accurate investigation into glass transition temperature (T_g), crystalline melting temperature (T_m),

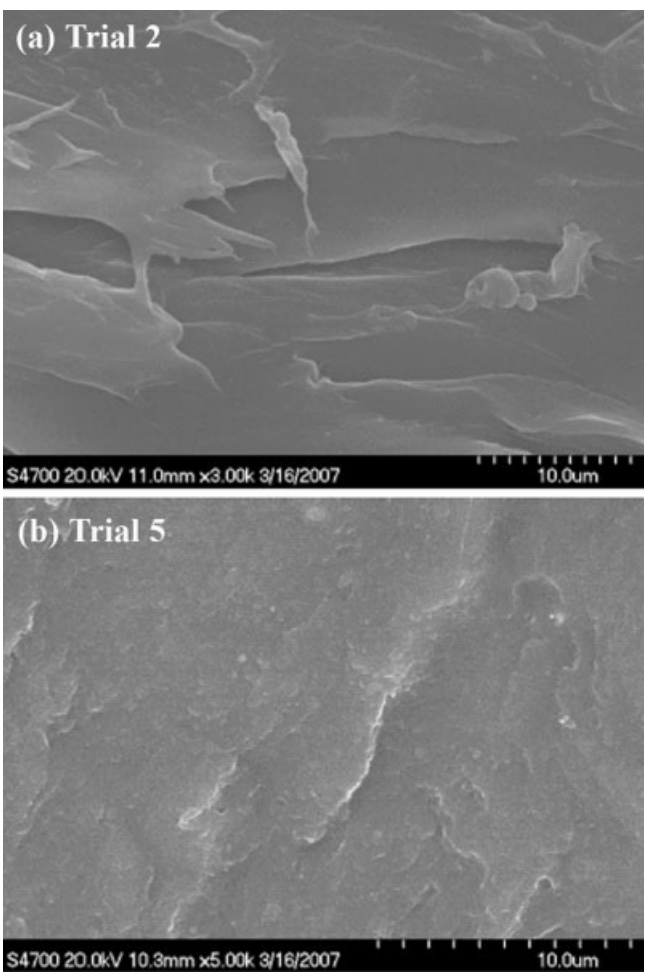

Figure 4 Morphologies of (a) Trial 2 and (b) Trial 5.

TABLE III
Influence of Polymeric Systems on Some Parameters

Trial	T_g[a] (°C)	T_m[b] (°C)	ΔH_f[c] (J/g)	χ_{DSC}[d] (%)	χ_{XRD}[e] (%)	T_d[f] (°C)	W_a[g] (%)
2	51.0	217.6	57.94	25.19	23.7	322	4.8
3	54.3	216.8	50.92	22.14	21.1	328	3.7
4	58.2	217.7	43.59	18.95	18.6	343	3.1
5	61.1	216.8	39.87	17.33	16.8	367	1.9

[a] Glass transition temperature.
[b] Melting temperature.
[c] Heat of fusion.
[d] Percentage crystallinity calculated by DSC analysis.
[e] Percentage crystallinity calculated by XRD analysis.
[f] Degradation temperature by TG analysis.
[g] Water absorption calculated by eq. (4).

and percentage crystallinity (χ_{DSC}) was presented by DSC analysis for polymers, and the detailed data are listed in Table III.

As shown in Figure 5, the T_g's of graft copolymers are higher than that of homo-PA6 (Trial 2). Here, PA6 chemically attaches upon the rigid PS backbone with a high T_g (about 100°C). It is speculated that the increase in T_g is due to the constrained mobility of PA6 chain. As the PS content increases (the PA6 length decrease), the magnitude of T_g increase became large. The single T_g, however, indicates that there is only one relatively homogeneous structure in the product, i.e., PS-*g*-PA6 copolymer. It is in agreement with the results from selective extraction.

The incorporation of PS into PA6 also shows heat capacity changes which could be assigned to the crystalline melting of PA6 (Fig. 6). Upon reheating, the variation of T_m of graft copolymers is less significant as the PS content increases; however, the onset melting point is shifted to lower temperature and the melting curve becomes broader. These variations can be attributed to the fine dispersion of PS phase in PA6 matrix (confirmed by SEM), which increases the disorder of system and destroys the crystallinity of PA6. The effect becomes more evident at higher PS content and induces forming more PA6 imperfect crystallites, resulting in the broadening of melting cure.

A careful observation of the crystalline melting cure of homo-PA6 (Trial 2) leads to the identification of γ type crystal of PA6, with a very weak shoulder endothermic peak at low temperature, while the main peak corresponds to the α type crystal.[18] PS-*g*-PA6 graft copolymers show the similar main and shoulder peaks (Trials 4 and 5).

The χ_{DSC} value of polymers was calculated via the ratio between the measured and equilibrium heats of fusion (Table III). The results show the χ_{DSC} value of graft copolymer is lower than that of homo-PA6 and decreases with increasing PS content (as also confirmed by XRD). This decreasing trend is due to the disruption of polyamide packing. As discussed earlier, well-proportioned PS segments are destroyers of

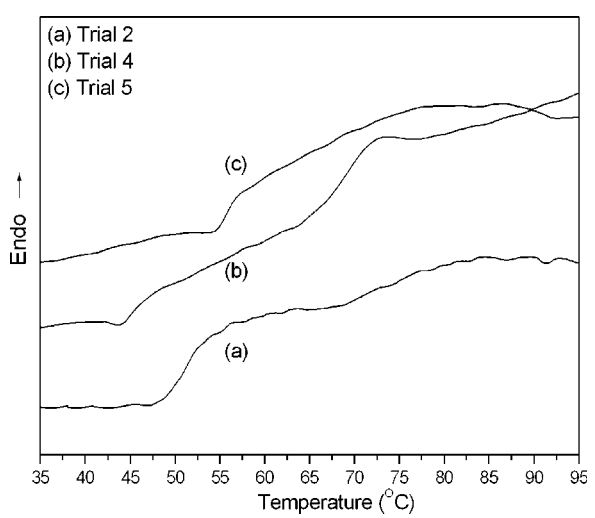

Figure 5 Glass transition of (a) Trial 2, (b) Trial 4, and (c) Trial 5.

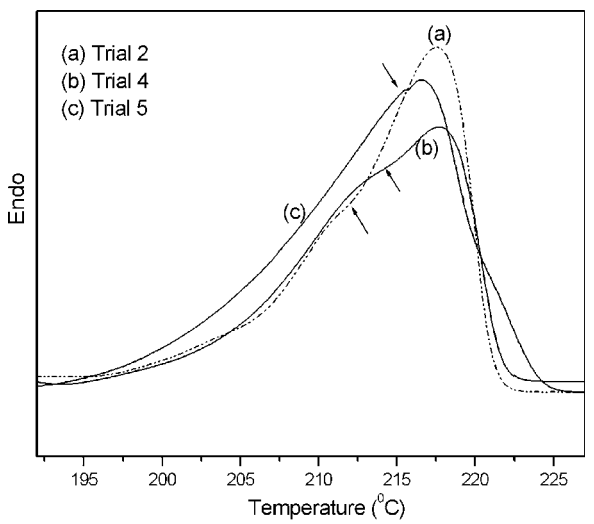

Figure 6 Crystalline melting of (a) Trial 2, (b) Trial 4, and (c) Trial 5.

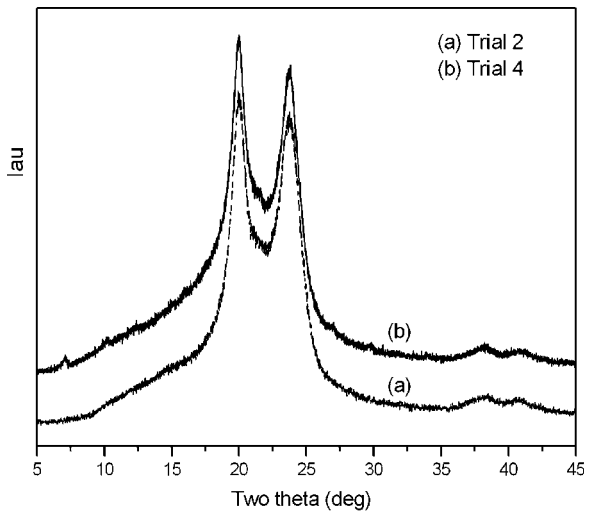

Figure 7 XRD patterns of (a) Trial 2 and (b) Trial 4.

the hydrogen bonding of polyamide. This effect becomes more evident at higher PS content.

XRD analysis

Figure 7 shows the XRD intensity profiles of homo-PA6 and PS-*g*-PA6 copolymer. The crystalline regions of homo-PA6 hold two characteristic peaks of PA6 α form at α_1 $2\theta = 20.0^\circ$ and α_2 $2\theta = 23.8^\circ$, corresponding to the reflections of the crystalline planes (200) and (002) + (202), respectively.[26] The XRD profile of PS-*g*-PA6 copolymer is analogous with that of homo-PA6, indicating that in the copolymer the crystal structure of PA6 is scarcely affected by the presence of PS. The PA6 γ form discussed in DSC Section, corresponding to the reflection of the crystalline plane (001), is not seen in the XRD pattern. This may be due to the variation of thermal and processing conditions between XRD and DSC.[27]

The percentage crystallinity discussed in DSC Analysis Section can also be described with XRD (χ_{XRD}) (Table III). There is an excellent agreement between the XRD and DSC estimates of crystallinity for all samples, although the DSC data are shifted to higher values. The good correspondence between the two sets of data supports the general conclusion drawn above.

TG analysis

TG analysis in a nitrogen atmosphere is used to evaluate the thermal degradation behavior of the copolymers. Typical TG diagrams and their differential forms are shown in Figure 8. Homo-PA6 has two weight loss regions, 300–360 and 400–450°C respectively. The first one is a result of the degradation of low molecular weight polyamides and oligomers, and the second/major region is due to the degradation of PA6 chain into low molecular weight substances.[23] For the PS-*g*-PA6 copolymer of Trial 4, the first region is inconspicuous, which indicates the incorporation of PS into PA6 slows down the degradation of PA6 at low temperature and contributes to the protection of PA6 matrix.

Degradation temperatures of polymers obtained by TG analysis (T_d, the temperature at which the sample lost 5% of its original weight) are listed in Table III. The results show the T_d value of PS-*g*-PA6 copolymer is higher than that of homo-PA6 and increases obviously with increasing PS content. Upon the incorporation of 18.3 wt % PS-CCL into the polymeric system, the T_d of Trial 5 is about 45°C higher than that of homo-PA6. The graft copolymer has improved thermal properties.

Water absorption

PA6 is semicrystalline and extremely sensitive to water absorption because of the existence of interchain hydrogen bonding sites between amide groups. This may cause dimensional instability with property degradation and ultimately lead to failure during its life exposure. To evaluate the dimensional stability of graft copolymers, water absorption measurement was conducted with polymer powers (about 10 g). The sample after selective extraction was dried at 60°C in an oven for 24 h and placed in a desiccator to cool. The sample was weighed (W_4), and then emerged in water at ambient temperature for 24 h. It was removed, patted dry with a lint free cloth, and weighed (W_5). Water absorption is expressed as increase in weight percent.

$$\text{Water absorption } (\%) = \frac{W_5 - W_4}{W_4} \times 100 \qquad (4)$$

For polyamides, the amount of water absorption commonly decreases with increasing the crystallin-

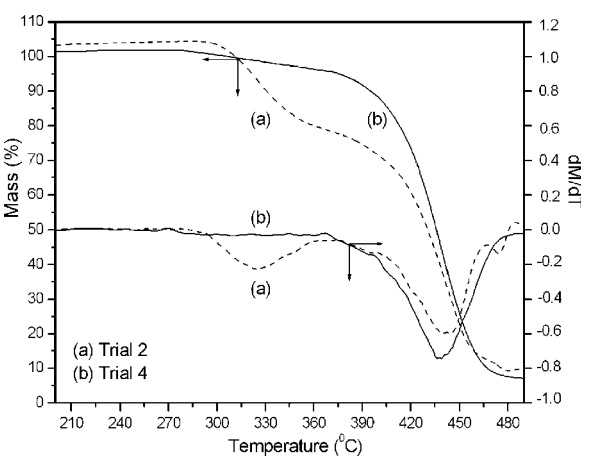

Figure 8 TG diagrams and their differential forms of (a) Trial 2 and (b) Trial 4.

ity. Water molecules can only diffuse into the amorphous phase, but they cannot penetrate into the crystal domain and break apart existing amide–amide bonds in this phase.[28] The water absorptions of PS-*g*-PA6 graft polymers listed in Table III, however, does not follow the above rule. As one can see, they are lower than that of homo-PA6, and decrease with increasing the PS content (decreasing the crystallinity). Here, as regards the water absorption mechanism of graft copolymers, another aspect expect for the percentage crystallinity should be taken into account: the hydrophobic nature of PS segment. As the PS content increases, the proportion of amide groups in amorphous decreases. Thus, the hydrophobic nature of PS is experimentally proved to be the major factor in resulting in the decrease of water absorption. The graft copolymer is postulated to own higher dimensional stability than homo-PA6.

CONCLUSIONS

PS-*g*-PA6 graft copolymers have been obtained by anionic polymerization of CL in the presence of PS-CCL macroactivators synthesized by free radical copolymerization of styrene and ACCL. The addition of PS-CCL in this study resulted in a polymerization time of less than 20 min. The results obtained by selective solvent extraction are in favor of the formation of graft copolymers with high purity. DSC analysis gives complementary information supportive of PS-*g*-PA6 formation by the single glass transition. SEM micrographs of fracture surfaces suggest that PS phase was well dispersed in PA6 matrix. The XRD experiments suggest that the addition of PS scarcely influences the crystalline structure of PA6. As the PS content increases, the water absorption and percentage crystallinity of graft copolymers decrease, but the glass transition temperature and degradation temperature increase. The PS-*g*-PA6 copolymer has better thermal properties and dimensional stability than homo-PA6.

The authors thank Prof. Changyuan Yu of Beijing University of Chemical Technology for his help in recording SEM micrographs, and State Key Laboratory of Chemo/Biosensing and Chemometrics for ^{1}H NMR analysis.

References

1. Freluchea, M.; Iliopoulos, I.; Millequant, M.; Flat, J. J.; Leibler, L. Macromolecules 2006, 39, 6905.
2. Freluchea, M.; Iliopoulos, I.; Flat, J. J.; Ruzette, A. V.; Leibler, L. Polymer 2005, 46, 6554.
3. Pae, Y. J Appl Polym Sci 2006, 99, 292.
4. Pae, Y. J Appl Polym Sci 2006, 99, 309.
5. Villarreal, M. E.; Tapia, M.; Nuno-Donlucas, S. M.; Puig, J. E.; Nunez, G. J. Appl Polym Sci 2004, 92, 2545.
6. Li, H.; Li, Z. Polym Int 1999, 48, 124.
7. Li, H.; Li, Z. J Appl Polym Sci 1998, 67, 61.
8. Fu, Q.; Livengood, B. P.; Shen, C.-C.; Lin, F.-L.; Li, W.; Harris, F. W.; Chen, S. Z. D.; Hsiao, B. S. J Polym Res 1997, 4, 1.
9. Carone, E.; Felisberti, M. I.; Nunes, S. P. J Mater Sci 1998, 33, 3729.
10. Liu, B.; Zhang, C.; Feng, L.; Xu, Z. Modern Plast Proc Appl 2005, 17, 6.
11. Crespy, D.; Landfester, K. Macromolecules 2005, 38, 6882.
12. Ricco, L.; Russo, S.; Orefice, G.; Riva, F. Macromolecules 1999, 32, 7726.
13. Mateva, R.; Filyanova, R.; Velichkova, R.; Gancheva, V. J Polym Sci Part A: Polym Chem 2002, 41, 487.
14. Petrov, P.; Gancheva, V.; Philipova, T. Z.; Velichkova, R.; Mateva, R. J Polym Sci Part A: Polym Chem 2000, 38, 4154.
15. Tsui, S. W.; Johnson, A. F. J Mater Sci 1995, 30, 5967.
16. Hu, G. H.; Li, H.; Feng, L. F. Macromolecules 2002, 35, 8247.
17. Liu, Y.-C.; Xu, W.; Xiong, Y.-Q.; Zhang, F.; Xu, W. J Mater Lett 2007, to appear.
18. Udipi, K.; Dave, R. S.; Kruse, R. L.; Stebbins, L. R. Polymer 1997, 38, 927.
19. Russell, D. P.; Beavmont, P. W. J Mater Sci 1980, 15, 197.
20. Mateva, R.; Petrov, P.; Rousseva, S.; Dimitrov, R.; Zolova, G. Eur Polym Mater 2000, 36, 813.
21. Marelova, J.; Roda, J.; Stehlicek, J. Eur Polym Mater 1999, 35, 145.
22. Stehlicek, J.; Baldrian, J.; Puffer, R.; Lednicky, F.; Dybal, J.; Kovarova, J. Eur Polym Mater 1997, 33, 587.
23. Zhang, C. L.; Feng, L. F.; Hu, G. H. J Appl Polym Sci 2006, 101, 1972.
24. Ueda, K.; Hosoda, M.; Matsuda, T.; Tai, K. Polym J 1998, 30, 186.
25. Omonov, T. S.; Harrats, C.; Groeninckx, G. Polymer 2005, 46, 12322.
26. Rusu, G.; Ueda, K.; Rusu, E.; Rusu, M. Polymer 2001, 42, 5669.
27. Yu, Y. C.; Jo, W. H. J Appl Polym Sci 1995, 56, 895.
28. Pae, Y. J Appl Polym Sci 2006, 99, 300.